Journal of
Chemical Engineering & Process Technology

Monmaturapoj, et al., J Chem Eng Process Technol 2015, 6:2
DOI: 10.4172/2157-7048.1000221

Research Article Open Access

Honeycomb Structures of TiO_2-modified Hydroxyapatite Composite for Microbial Filtration Application

Naruporn Monmaturapoj*, Witoon Thepsuwan, Suda Wanakitti, Charusporn Mongkolkachit, Katanchalee Mai-ngam, Sawinee Ngernpimai, Wattana Klinsukhon and Chureerat Prahsarn

National Metal and Materials Technology Center, 114 Thailand Science Park, Pathumthani 12120, Thailand

Abstract

Honeycomb structures of TiO_2-modified hydroxyapatite composite (HA/TiO_2) were fabricated using extrusion technique. The mixture formulations of HA/TiO_2 extrusion pastes (S1-S4) were investigated to optimize the process. The filtering effectiveness of the HA/TiO_2 honeycombs was evaluated by photocatalytic activity measurement and a bactericidal test. The effects of sintering temperature and honeycomb thickness on photocatalytic and antibacterial activities were additionally studied. The S3 and S4 honeycomb samples, sintered at 650°C, exhibited a similar trend in reducing methylene blue concentration. At 800°C, the S3 honeycomb sample showed a slightly faster reduction in methylene blue concentration compared to the S4 honeycomb. Honeycomb samples of 2 and 5 cm in thickness showed significantly greater photocatalytic activity than that of 1 cm such that methylene blue concentrations rapidly decreased after UV exposure for 24 hours. The S3 and S4 honeycomb samples also exhibited decomposition of both gram-negative *E. coli* and gram-positive *S. aureus*. Approximately 50% of gram-positive *S. aureus* and gram-negative *E. coli* were decomposed by the honeycombs in the sample-thickness dependent manner after 2 hours of UV exposure. Low survival ratios of bacteria (5% - 10%) were observed after 6 hours of UV exposure and the 2 mm and 5 mm thick honeycomb samples showed the greatest and most similar antibacterial activities.

Keywords: Honeycomb; Hydroxyapatite; Titanium dioxide; Antibacterial; Photocatalytic activity

Introduction

Hydroxyapatite (HA, $Ca_{10}(PO_4)_6(OH)_2$), a calcium phosphate based compound which closely resembles natural bones and teeth, has been extensively used for biomedical applications, particularly for replacing human hard tissue [1-6]. It possesses excellent osteoconductivity, bioactivity, ionic exchange property and high stability under reducing and oxidizing situations leading to the adsorption ability for microbial bacteria and viruses [7-10]. HA is capable of adsorbing molecules on its surface but not decomposing molecules nor making microbes harmless, therefore, saturation will be reached over time [11].

Nanoparticle titanium dioxide (TiO_2) is a basic material extensively utilized in daily life, for example, as a pigment for paints, cosmetics and foodstuffs because of its effective performance as a photocatalyst. It is of great interest due to its potential in the oxidative decomposition of organic compounds, strong oxidizing power under UV, chemical stability, non-toxicity and long-term stability against photo and chemical corrosion [7-12]. However, TiO_2 can decompose only substances that come into direct contact, and the decomposition requires the presence of light, especially in the ultraviolet range [13-15]. By modifying the HA with TiO_2, their advantages can be combined-the HA adsorbs molecules that will then later be decomposed by TiO_2. The HA/TiO_2 composite has, therefore, the potential to be used for solving environmental problems such as water and air pollution due to its photocatalytic, antibacterial and antivirus properties. Nishikawa et al. reported that HA/TiO_2 composite exhibited higher photocatalytic activity than commercial TiO_2 and showed the rapid and complete oxidative decomposition of acetaldehyde [16]. The use of HA/TiO_2 composite as a bone scaffold coupled with collagen type I in the form of nanofiber mats fabricated by the electro spinning technique has also been reported [17]. Coating of hydroxyapatite on titania has been reported for bone substitute application [18]. Moreover, the composite of HA/TiO_2 can be applied in the field of sonocatalysis to damage bovine serum albumin (BSA) under ultrasonic irradiation [19].

At present, for the filtration application, most research has concentrated on coating the thin film of HA/TiO_2 composite onto substrate materials. However, the photocatalytic activities of the HA/TiO_2 particles coated on the substrate decreased compared to those in powder form, due to a decrease in the surface area of the particles. In addition, coating the HA/TiO_2 composite onto fibrous substrates for microbial filter application was also reported to have limitations in use. In the coating, particles can either deposit onto the fibers' surfaces or penetrate into the inter-fiber space which may not be fully exposed to UV light. The latter could lead to a decrease in photocatalytic activity [20]. By forming HA/TiO_2 composites into porous structures, which provide higher surface area and increase exposure area to UV light, it is possible to increase photocatalytic efficiency.

Honeycomb is a complex structure composed of several small unit cells, which have a thin wall between each cell. Honeycomb ceramics are widely used as a catalytic converter in automobile gas exhausts and a catalyst carrier [21]. Ceramic honeycomb structures provide the high surface areas with least volume. The geometric surface area of the carrier due to the characteristics of the porous thin wall greatly increased and improved thermal shock resistance [22,23]. Industrially, extrusion is one of the most popular techniques with which to fabricate honeycomb ceramics. Many factors influencing the properties of the final honeycomb products, particularly the compositions of raw materials, need to be controlled to achieve the desirable products.

***Corresponding author:** Naruporn Monmaturapoj, National Metal and Materials Technology Center, 114 Thailand Science Park, Pathumthani 12120, Thailand, Tel: 662564 6500; E-mail: naruporn@mtec.or.th

Received March 30, 2015; **Accepted** April 08, 2015; **Published** April 16, 2015

Citation: Monmaturapoj N, Thepsuwan W, Wanakitti S, Mongkolkachit C, Mai-ngam K et al. (2015) Honeycomb Structures of TiO_2-modified Hydroxyapatite Composite for Microbial Filtration Application. J Chem Eng Process Technol 6: 221. doi:10.4172/2157-7048.1000221

In this study, extrusion technique was employed to fabricate HA/TiO_2 composite at a ratio between HA to TiO_2 of 50:50 by weight. Four different mixture formulations of extrusion pastes were investigated in order to fabricate HA/TiO_2 honeycombs. The effects of sintering profiles and honeycomb thickness on photocatalytic activity and bactericidal performance were investigated and discussed in terms of their potential uses as microbial filters.

Experimental Procedure

Preparation and characterization of pure hydroxyapatite (HA)

Pure hydroxyapatite was prepared using a solid-state reaction method. Mixture powders of calcium carbonate ($CaCO_3$) and calcium phosphate dibasic ($CaHPO_4$) reacted as shown in equation (1).

$$4CaCO_3+6CaHPO_4 \rightarrow Ca_{10}(PO_4)_6(OH)_2+2H_2O+4CO_2 \quad (1)$$

All raw materials were used as received. $CaCO_3$ (Carlo Erba Reagenti, Italy) and $CaHPO_4$ (Sigma-Aldrich, Germany) were ball-milled with zirconia balls in the presence of deionized water as a medium for 48 hours, before drying. The mixture was then calcined at 900°C for 2 hours to produce pure hydroxyapatite powder. The obtained powders were ground and sieved to attain a particle size of less than 10 μm. Characterization of HA powders after calcination was done using x-ray diffraction: XRD (JEOL JDX 3530) with CuK_α source (K_α = 1.5406 nm) operating at 30 mA and 50 kV. XRD measurement was conducted at 20-60° 2θ, scan speed of 2°/min with a step size of 0.02°. The XRD spectra were analyzed using JADE software and ICDD cards. Particle size analysis was measured by laser diffraction technique (Mastersizer 2000, Malvern instruments, UK).

Preparation and characterization of HA/TiO2 composite

Anatase phase TiO_2 (Sigma-Aldrich, Germany) was used as received. HA/TiO_2 composite was prepared by dry ball milling the mixture between HA and TiO_2 powders at the composition ratio of 50:50 (HA: TiO_2 50:50), using ZrO_2 balls for 3 hours. The obtained HA/TiO_2 composite was then calcined at 650°C for 2 hours. The composite was then wet milled for another 24 hours using deionized water as the medium under ZrO_2 balls to achieve a particle size of less than 5 micron, followed by drying at 100°C. The particle size of HA/TiO_2 composite was analyzed by laser diffraction technique (Mastersizer 2000, Malvern instruments, UK). Analysis of their phases was carried out using XRD: JEOL JDX 3530.

Preparation and characterization of honeycomb structure

Four different mixture formulations of the extrusion pastes (S1-S4) as summarized in Table 1 were prepared for fabricating the HA/TiO_2 honeycombs. The paste compositions consisted of HA/TiO_2 composite powder as the main component, processing additives which were water as medium, methylcellulose (MC) and starch as binders, polyethylene glycol (PEG) and flour as plasticizers, sodium carbonate as a dispersant as well as some lubricants such as oil. Each formulation was uniformly mixed using a high speed mixer before being further transferred to a 3-roll mill for homogenous mixing. These paste batches were then de-aired and extruded using a screw extruder (FM-30, Miyazaki Iron Work, Japan) into cylindrical honeycomb structures of 50 mm in diameter with a cell density of 72 cell/inch^2 and having three different thicknesses (1, 2 and 5 cm). The extruded HA/TiO_2 honeycomb samples were covered with semi-dry cloth to let them slowly dry at room temperature. After drying, the honeycomb samples of selected formulations, S3 and S4, were sintered at 400°C for 2 hours and then ramped up to three different temperatures (650, 800 and 1000C) held for 4 hours, followed by furnace cooling to room temperature at a rate of 50°C/h. Phases and microstructures of the obtained HA/TiO_2 honeycombs were analyzed using XRD: JEOL JDX 3530 and scanning electron microscopy (SEM: JEOL JSM-5410).

Physical and mechanical properties

Five specimens each of S3 and S4 honeycomb structures, sintered at 650°C and 800°C, were used to measure bulk density and total porosity based on Archimedes' principle. The honeycombs were dried in an oven at 100°C and cooled to room temperature before testing. In accordance with Archimedes' principle, a sample was completely dried and then weighed . The weight was recorded as W_d. After weighing, the sample was placed in a beaker with the deionized (DI) water to allow the specimen to be soaked in the water for 24 hours. Within 24 hours, the specimen was assumedly saturated and then a vacuum was applied to force the water into the open pores of the honeycomb structures until no air bubbles emerged from the structure. After that, the beaker was placed on a stand over a balance. A density kit was hung below the water level but not touching any sides of the beaker in a position ready to determine the density of the sample. The sample was lifted onto the wire and the suspended weight was recorded as W_s. Finally, the sample was removed from the water, rapidly blotted, and weighed to attain the saturated weight, W_w. The bulk density of the sample, D_b, was calculated as

$$D_b = \frac{W_d \times \rho_w}{W_w - W_s} \quad \text{where } \rho_w = 1 \text{ g/cm}^3 \text{ at } 25°C$$

The total porosity of sample, P_t was evaluated as

$$P_t = \frac{(D_t - D_b)}{D_t}$$ where D_t is the theoretical density of HA/TiO_2 (50:50) composite (3.468 g/cm^3)

For mechanical properties testing, the specimen was prepared by extruding HA/TiO_2 composites into bars (6 mm wide x 5 mm long) and sintered at 650°C and 800°C. The 3-point bending strength of the sintered specimen was tested using a universal testing machine (Instron 55R4502, USA) with 10kN load cells. The crosshead speed was set at 0.5 mm/min and the span length to 20 mm. Five specimens were tested to obtain average values and standard deviations.

Investigation of photocatalytic activity

The photocatalytic activities of HA/TiO_2 honeycomb structures were investigated by measuring the degradation of methylene blue (MB) under UV irradiation. For comparison, MB solution without honeycomb sample was used as a blank. The evaluation was conducted

Sample	HA/TiO_2	DI water	MC	PEG	Na_2CO_3	Oil	Starch	Flour
S1	63.45	22.46	5.08	2.54	0.76	5.71	-	-
S2	59.95	21.58	9.59	0.36	0.24	5.28	2.99	-
S3	57.47	22.99	10.34	0.92	0.23	5.17	2.87	-
S4	55.07	25.88	8.81	0.66	0.22	4.96	-	4.40

Table 1: Formulations of extrusion paste studied in this work (%wt).

in a closed chamber equipped with UV-A lamps (315-380 nm). 250 mL of 5 ppm MB solution was added into a beaker, and the sample was put into the prepared MB solution. The beaker was placed into chamber and dark closed (no UV light) for 1 hour for initialization. Then, the MB solution was sampled out and measured for UV absorption (600-700 nm) on a UV spectrophotometer (JASCO-V530) and the absorption at peak (665 nm) was used to determine MB concentration at initial time (t_0). UV lamps in the chamber were then turned on to allow photocatalytic activity. After 1 hour, the lamps were turned off and MB concentration at the testing time of 1 hour (t_1) was determined. The same procedure was continued for other exposure times (1, 3, 6, and 24 hours) to determine the corresponding MB concentrations at t_1, t_3, t_6, and t_{24}.

Antibacterial Activity Test

Two types of bacteria, *E. coli* ATCC 8739, a Gram-negative bacterium, and *S. aureus* ATCC 6538, a Gram-positive bacterium, were chosen as model microorganisms in this study. Both bacteria, stored in glycerol at -80°C, were plated on nutrient agar, a mixture of nutrient broth (NB) and Bacto agar (Difco), cultured overnight at 37°C for 24 hours and stored at 4°C. Prior to each experiment, the strains were inoculated in sterile test tubes in NB and cultured at 37°C for 12 hours in order to reach the stationary growth phase. The cultures were harvested by centrifugation and resuspended in phosphate buffered saline (PBS, pH 7.4) to OD600 of 0.4, corresponding to an approximate concentration of 10^8 colony-forming units (cfu)/mL.

Honeycomb specimens were autoclaved and kept separate until use in a sterile beaker. The bacterial suspension (40, 60 and 100 mL) was added to the honeycomb samples sized 1, 2 and 5 cm, respectively and kept under 6-watts UV lamp illumination for 2, 4 and 6 hours with an approximate distance of 65 cm between the specimens and the lamp. *E. coli* suspension was removed at 2, 4 and 6 hours. Viable concentration of *E. coli* was enumerated using the spreading plate method on nutrient agar (NA) after a series of dilutions of the sample in normal saline. A 100 µl bacterial suspension was removed at 4-hour intervals and spread onto the nutrient agar medium and incubated for 24 hours to determine the number of viable cells. The efficacy of the antimicrobial activity is expressed as: survival ratio (%) = N/N_0 x 100, where N is number of survival bacteria and N_0 is the number of original bacteria. Experiments with bacterial cultures without honeycomb sample were conducted as controls. The mean and standard deviation from triplicate samples were indicated. In addition, a survival ratio curve for a 48-hour culture period was completed by combining two data sets in order to avoid working at night.

Results and Discussion

Effect of paste formulations on Hydroxyapatite/Titania honeycomb structures

In extrusion of HA/TiO_2 honeycomb structures, processing additives such as binders, plasticizers and lubricants were added to improve the plasticity and extrudability of the non-plastic HA/TiO_2 powders. By employing different paste formulations (Table 1), it was found that different pressure was required for extruding the samples due to the different textures in each formulation. The S3 and S4 formulations, which yielded complete shapes of honeycomb structure with sufficient green strength and good handling characteristics, were chosen for further investigation in the next step. Example images of final honeycomb structures of S3 samples after sintering at 800°C for 4 hours with different thickness are shown in Figure 1.

Characterization and mechanical properties

Figure 2 shows the XRD patterns of as-synthesized HA, TiO_2, and HA/TiO_2 honeycombs (as-prepared, and after sintering at 650, 800 and 1000°C). XRD patterns confirmed presence of all expected major hydroxyapatite (JCPDS No. 09-0432) and anatase TiO_2 (JCPDS No. 21-1272) crystallizations in the synthesized HA and TiO_2 used as raw materials, respectively.

The mixture of hydroxyapatite and anatase TiO_2 phases can be indexed in the as-prepared honeycombs and after sintering at 650°C. No additional phase associated with either decomposition of HA to β-tricalcium phosphate (β-TCP) or transformation of anatase to rutile TiO_2 was observed in the honeycomb sintered at this temperature. As expected, for HA/TiO_2 honeycomb sintered at 800°C, few small peaks of β-TCP due to the decomposition of HA into β-TCP as well as the peaks of the anatase phase of TiO_2 were observed. Generally, HA can decompose into β-TCP at a sintering temperature range of 800-1350°C [2,24,25]. With increasing sintering temperature, HA tended to completely decompose into β-TCP coupled with more transformation of anatase to rutile of TiO_2. The peaks related to $CaTiO_3$ were also observed due to the reaction between TiO_2 and Ca^{2+} in the hydroxyapatite site, particularly at a sintering temperature of 1000°C. As a photocatalyst, anatase TiO_2 exhibited higher photocatalytic activity than other phases of TiO_2 (rutile and brookite) [7-12]. The high intensity of peaks relating to the anatase TiO_2 observed in the prepared HA/TiO_2 composite powder implied superior crystalline size and high crystallinity. The optimal sintering temperature range of 600°C to 950°C for TiO_2 had been reported to avoid the transition of anatase to

Figure 1: Honeycomb structures of S3 of different thicknesses after sintering at 800°C for 4 hours.

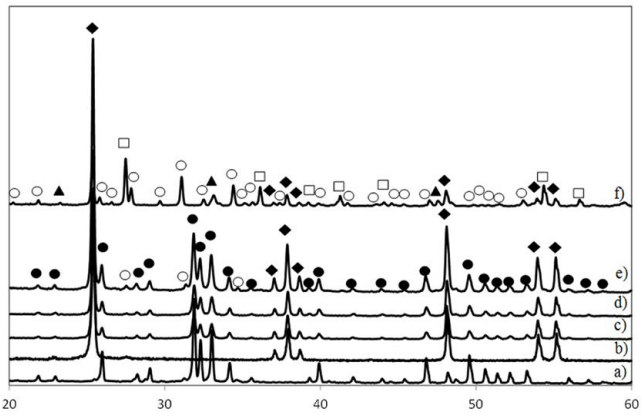

Figure 2: XRD patterns of a) as-synthesized HA, b) anatase, TiO_2, c) as-prepared HA/Ti composite, honeycomb sintering at d) 650°C, e) 800°C and f) 1000°C. • Hydroxyapatite, ♦ anatase TiO_2, □ rutile, TiO_2, ○ β-TCP and ▲ $CaTiO_3$.

rutile [26-28]. Therefore, the sintering temperatures 650°C and 800°C were selected for further investigation in this study.

The influence of sintering temperature on the morphology of HA/TiO_2 honeycombs was investigated. In this step, S3 and S4 formulations, which yielded complete shapes of honeycomb structure, were employed. Figure 3 illustrates the morphology of the honeycomb structure. Overall, irregular shapes of HA and TiO_2 crystals were observed in which small crystals of anatase TiO_2 were distributed and embedded in larger HA crystals with micropore sizes in the range of 0.23-0.28 μm. Similar morphologies were observed in honeycombs sintered at 650 and 800°C. Meanwhile, honeycomb samples sintered at 1000°C exhibited larger pore sizes (~0.40 μm) compared to those sintered at 650°C and 800°C. HA/TiO_2 grain size increased with sintering temperature, thus resulting in the decrease in porosity.

From the results shown earlier (Figure 2), honeycombs sintered at 1000°C exhibited transformation from anatase to rutile TiO_2 whereas those sintered at 650°C and 800°C did not. Therefore, the honeycombs sintered at 650°C and 800°C were chosen for further investigation on the properties of HA/TiO_2 honeycombs such as strength, photocatalytic activity, and anti-bacterial performance.

Table 2 presents the bulk density and total porosity of the S3 and S4 honeycomb structures of different sintering temperature and thickness. A small discrepancy in density (~30%) and porosity (~60%) was observed among S3 and S4 samples sintered at 650°C and 800°C. It seems that samples sintered at 800°C exhibited a slightly higher density, particularly in the thick samples (5 cm). It might be difficult to clearly determine the density and porosity of the honeycomb structure using Archimedes' principle, compared to SEM images, due to the limitations of the technique and the complexity of the honeycomb structure itself. Therefore, neither a trend of increasing nor decreasing for both density and porosity could be clearly identified with sintering temperature.

The bending strength of honeycomb structures sintered at 650°C and 800°C are reported in Table 3. The honeycombs sintered at 800°C possessed a greater bending strength than those sintered at 650°C due to higher densification and less porosity, in micro scale, as evidenced by the SEM images (Figure 3). This implies that the strength of the honeycomb could be improved by increasing the sintering temperature. At a higher sintering temperature (1000°C), however, the phase transformation from anatase to rutile occurred and could reduce the desired photocatalytic activity.

Photocatalytic activity

The photocatalytic activities of S3 and S4 HA/TiO_2 honeycombs of thickness 1, 2, and 5 cm sintered at 650°C and 800°C were evaluated using 5 ppm MB solution. According to the results, the

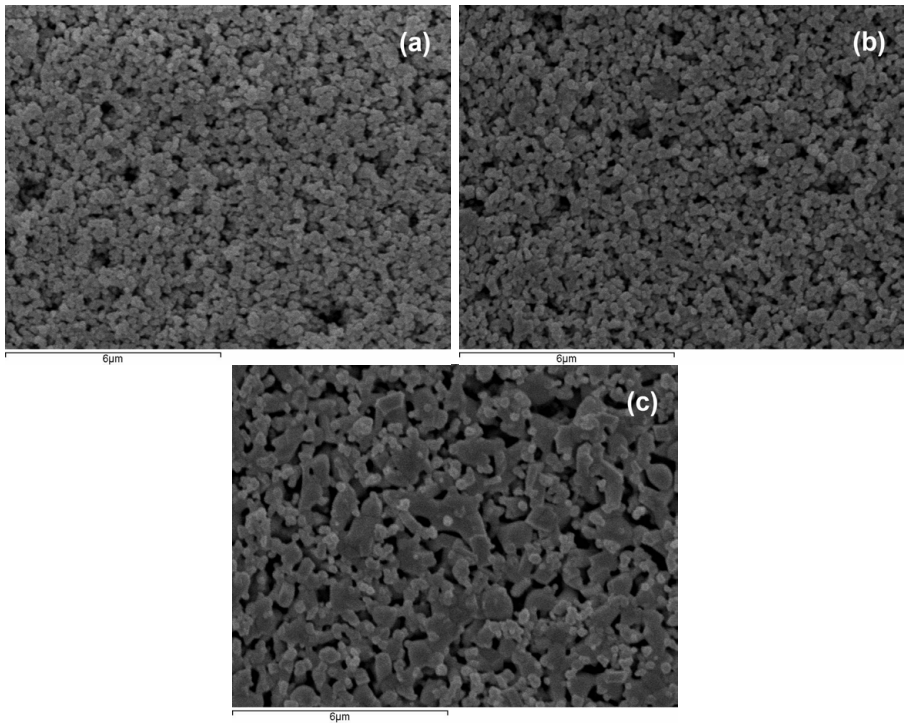

Figure 3: Morphology of honeycomb samples after sintering at a) 650°C, b) 800°C and c) 1000°C (heating rate of 50°C/h).

Formulation	Temperature (°C)	Density (%) ± SD.			Porosity (%) ± SD.		
		Thickness (cm)			Thickness (cm)		
		1	2	5	1	2	5
S3	800	33.97 ± 1.26	34.23 ± 1.34	36.21 ± 0.82	62.72 ± 1.38	62.43 ± 1.47	60.26 ± 0.90
S4	650	32.62 ± 0.78	35.30 ± 1.17	34.78 ± 1.34	64.20 ± 0.86	61.26 ± 2.24	61.83 ± 1.47
	800	33.44 ± 1.41	31.81 ± 0.90	34.89 ± 0.64	63.30 ± 1.55	65.09 ± 0.99	61.71 ± 0.71

Table 2: Density and porosity of honeycomb samples.

Formulation	Maximum Flexural Strength (MPa)	
	800°C / rate 50 °C/h	650°C / rate 50°C/h
S1	7.17 ± 1.79	-
S2	9.51 ± 1.00	-
S3	9.29 ± 1.01	4.84 ± 0.33
S4	6.91 ± 1.55	4.38 ± 0.28

Table 3: Bending strength of all samples.

MB concentration decreased with UV exposure time in the presence of HA/TiO_2 honeycombs and the rate of MB decomposition was rapid during the first 3 hours, whereas the blank (without HA/TiO_2 sample) showed no significant change in concentration (Figures 4a and 4b). Overall, HA/TiO_2 honeycombs sintered at 800°C tended to show slightly higher rates of MB decomposition than those sintered at 650°C. This may be related to the higher intensities of anatase TiO_2 peaks observed in the HA/TiO_2 honeycomb sintered at 800°C (Figure 2e). The difference, however, was not significant. The S3 and S4 honeycombs exhibited comparable rates of MB decomposition. At the same sintering temperature, HA/TiO_2 honeycombs of thickness 2 and 5 cm exhibited comparable rates of MB decomposition, but slightly greater than that of the 1-cm thick honeycomb ($p<0.07$). The lower initial MB concentration (at 0 hr) of 5-cm thick honeycomb, compared to those of the 1 and 2 cm thick samples, was thought to be due to its greater area for MB adsorption during initialization. After 24 hours of UV exposure, the MB solutions in the presence of the HA/TiO_2 honeycombs were effectively decomposed as the solution became clear.

Antibacterial activity

A photocatalytic decomposition reaction of our HA/TiO_2 has been previously reported to be applicable to deactivate microorganisms under weak UV light [20]. In this study, the *in vitro* antibacterial activities of the S3 and S4 HA/TiO_2 honeycombs of different thicknesses under room ambience with UV light were investigated. The S3 and S4 HA/TiO_2 honeycombs were prepared from two similar compositions of extrusion paste that differed in the additive selection (Table 1). Figures 5a and 5b, respectively, show the curves of survival ratio (%) versus culture time for the HA/TiO_2 honeycombs against gram-positive *S. aureus* and gram-negative *E. coli*. The smaller the survival ratio, the higher the antibacterial activity of the sample. The survival ratios of both bacterial strains decreased with incubation time for all tested HA/TiO_2 honeycombs. The S3 and S4 honeycombs exhibited comparable antimicrobial activity as their survival curves with similar sample lengths could almost be superimposed for both *S. aureus* and *E. coli*. This may be explained by both the starch and flour respectively selected for the S3 and S4 honeycombs as processing additives being generally neither bactericidal nor bacteriostatic agents. Moreover, their other compositions were almost quantitatively and qualitatively similar.

At the UV exposure time of 2 hours, the survival ratios of both bacterial strains found for the S3 and S4 honeycombs significantly decreased as the sample length increased ($p < 0.003$). The explanation for this is that the longer the sample, the more the HA/TiO_2 photocatalyst is incorporated into the sample and the faster its bactericidal activity is initiated. At longer exposure times (4 and 6 hours), only 5 - 15 % of bacteria remained in a proliferative state and the 1-cm thick honeycomb samples, containing the least amount of HA/TiO_2, still showed the highest survival ratios, as compared to the corresponding 2 and 5 cm thick samples ($p<0.003$ for *S. aureus* and $p<0.001$ for *E. coli*). However, the bactericidal activities of the 2 and 5 cm thick samples after 4 and 6 hours exposure became statistically comparable ($p<0.088$ for *S. aureus* and $p<0.700$ for *E. coli*).

Conclusion

The honeycomb structures of TiO_2-modified hydroxyapatite (HA/TiO_2) composite were successfully fabricated through the extrusion method. The complete honeycombs of 50 mm in diameter and cell density of 72 cell/inch^2 were extruded in three different thicknesses (1, 2 and 5 cm). Fabrication of honeycomb structure requires a slow and consistent drying process before sintering. The appropriate sintering temperatures were 650 or 800°C. At these temperatures, the crystallizations of hydroxyapatite and anatase TiO_2, which were required for better photocatalytic and antibacterial activities as well as stronger samples, were achieved.

HA/TiO_2 honeycombs sintered at 800°C exhibited slightly higher photocatalytic activity, compared to those sintered at 650°C, due to the greater amount of anatase TiO_2. The S3 and S4 honeycombs exhibited comparable rates in reducing methylene blue concentration. For the same sintering temperature, the 2- and 5-cm thick honeycombs showed greater photocatalytic activity than that of the 1-cm thick honeycomb.

Antibacterial activity testing results reported that 50% of bacteria were decomposed after 2 hours of testing. With increasing culture time, less numbers of bacteria could survive -around 5-10% of bacteria survived after 6 hours of culture time. The S3 honeycomb sample did not exhibit significantly higher decomposition of both gram-negative *E. coli* and gram-positive *S. aureus* compared to S4. The thickness of the honeycomb samples also influenced the antibacterial performance of the samples for both *E. coli* and *S. aureus*. It has been found that 2cm and 5cm honeycomb samples showed greater antibacterial activity than the 1cm-honeycomb through the culture period of time.

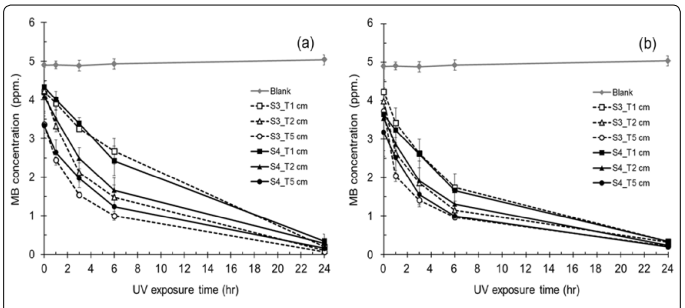

Figure 4: Methylene blue concentration after different UV exposure times in the presence of S3 and S4 HA/TiO_2 honeycombs with different thicknesses sintered at a) 650°C and b) 800°C

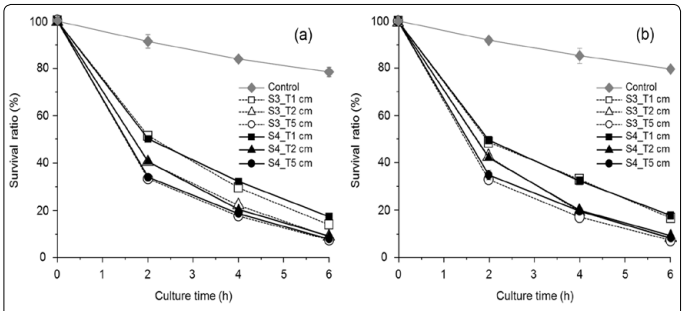

Figure 5: Antibacterial activities of the S3 and S4 HA/TiO_2 honeycombs with different thicknesses a) *E. coli* and b) *S. aureus*.

Acknowledgements

This work was performed with the support of the National Metal and Materials Technology Center, the Ministry of Science and Technology of Thailand, Project No. P-1200966.

There is no financial or other relationship that might be perceived as leading to a conflict of interest.

The authors declare that there are no conflicts of interest.

References

1. Hench LL (1991) Bioceramics: from concept to clinic. J Am Ceram Soc 74: 1487-1510.
2. Legeros RZ, Legeros JP (1993) Dense hydroxyapatite: An Introduction to Bioceramics. (1stedn), World Scientific, London.
3. Huang J, Best SM, Bonfield W, Buckland T (2010) Development and characterization of titanium-containing hydroxyapatite for medical applications. Acta Biomater 6: 241-249.
4. Wang CK, Ju CP, Lin JH (1998) Effect of doped bioactive glass on structure and properties of sintered hydroxyapatite. Mater Chem Phy 53:138-149.
5. Ramay HR, Zhang M (2003) Preparation of porous hydroxyapatite scaffolds by combination of the gel-casting and polymer sponge methods. Biomaterials 24: 3293-3302.
6. Saiz E, Gremillard L, Menendez G, Miranda P, Gryn K, et al. (2007) Preparation of porous hydroxyapatite scaffolds. Mat Sci and Eng C 27: 546-550.
7. Wakamura M (2005) Photocatalysis by calcium hydroxyapatite modified with Ti (IV). FUJITSU Sci Tech J 41: 181-190.
8. Fujishima A, Honda K (1971) Electrochemical evidence for the mechanism of the primary stage of photosynthesis. Bull Chem Soc Jpn 44: 1148-1150.
9. Fujishima A, Honda K (1972) Electrochemical photolysis of water at a semiconductor electrode. Nature 238: 37-38.
10. Ji S, Murakami S, Kamitakahara M, Ioku K (2009) Fabrication of titania/hydroxyapatite composite granules for photo-catalyst. Mater Res Bull 44: 768-774.
11. Anmin H, Ming L, Chengkang C, Dali M (2007) Preparation and characterization of a titanium-substituted hydroxyapatite photocatalyst. J Mol Catal A Chem 267: 79-85.
12. Ye FX, Ohmori A,Tsumura TT, Nakata K, Li CJ (2007) Microstructural analysis and photocatalytic activity of plasma-sprayed titania-hydroxyapatite coatings. J Therm Spray Tech 16: 776-782.
13. Lee MS, Hong SS, Mohseni M (2005) Synthesis of photocatalytic nanosized TiO_2-Ag particles with sol-gel method using reduction agent. J Mol Catal A Chem 242: 135-140.
14. Liu Y, Liu CY, Wei JH, Xiong R, Pan CX, et al. (2010) Enhanced adsorption and visible-light-included photocatalytic activity of hydroxyapatite modified Ag-TiO_2 powders. App Sur Sci 256: 6390-6394.
15. Nosaka Y, Matsushita M, Nishino J, Nosaka AY (2005) Nitrogen-doped titanium dioxide photocatalysts for visible response prepared by using organic compounds. Sci Tech Adv Mater 6: 143-148.
16. Nishikawa H, Kato S, Ando T (2005) Rapid and complete oxidation of acetaldehyde on TiO_2 photocatalytic filter supported by photo-induced activated hydroxyapatite. J Mol Catal A Chem 236: 145-148.
17. Kim HM, Chae WP, Chang KW, Chun S, Kim S, et al. (2010) Composite nanofiber mats consisting of hydroxyapatite and titania for biomedical applications. J Biomed Mater Res B Appl Biomater 94: 380-387.
18. Nayak S, Satpati B, Shukla KR, Dhawan A, Bhattacharjeea S, et al. (2010) A Facile synthesis of nanostructured hydroxyapatite–titania bio-implant scaffolds with different morphologies: their bioactivity and corrosion behavior. J Mater Chem 20: 4949-4954.
19. Jin X, Guo Y, Wang J, Wang Z, Gao J, et al (2011) The preparation of TiO_2/hydroxylapatite (TiO2/HA) composite and sonocatalytic damage to bovine serum albumin (BSA) under ultrasonic irradiation. J Molecular Catalysis A: Chemical 341: 89-96.
20. Monmaturapoj N, Thepsuwan W, Mai-Ngam K, Ngernpimai S, Klinsukhon W, et al (2014) Preparation and properties of hydroxyapatite/titania composite for microbial filtration application. Adv Appl Ceram 113: 267-274.
21. Suarez S, Yates M, Avila P, Blanco J (2005) New TiO_2 monolithic supports based on the improvement of the porosity. Catal Today 105: 499-506.
22. Ceramic Honeycomb Substrate
23. Ceramic honeycomb
24. Ou SF, Chioub SY, Ou KL (2013) Phase transformation on hydroxyapatite decomposition. Ceram Inter 39: 3809-3816.
25. Wang PE, Chaki TK (1993) Sintering behavior and mechanical properties of hydroxyapatite and dicalciumphosphate. J Mater Sci: Mater In Med 4: 150-158.
26. Suresh C, Biju V, Mukundan P, Warrier KGK (1998) Anatase to rutile transformation in sol-gel titania by modification of precursor. Polyhedron 17: 3131-3135.
27. Zhang Q, Gao L, Guo J (2000) Effects of calcination on the photocatalytic properties of nanosized TiO_2 powders prepared by $TiCl_4$ hydrolysis. Appl Catalysis B: Environmental 26: 207-215.
28. Hofer M, Penner D (2011) Thermally stable and photocatalytically active titania for ceramic surfaces. J Eur Ceram Soc 31: 2887-2896.